Fluorescence line narrowing-Zeeman spectroscopy of Cr^{3+}-doped $Gd_3Sc_2Al_3O_{12}$ garnet crystals

1992 J. Phys.: Condens. Matter 4 7307

(http://iopscience.iop.org/0953-8984/4/35/013)

J. Phys.: Condens. Matter 4 (1992) 7307–7316. Printed in the UK

Fluorescence line narrowing–Zeeman spectroscopy of Cr^{3+}-doped $Gd_3Sc_2Al_3O_{12}$ garnet crystals

Y Gao, M Yamaga†, C Ogihara‡, K P O'Donnell and B Henderson
Department of Physics and Applied Physics, University of Strathclyde, Glasgow G4 0NG, UK

Received 1 May 1992

Abstract. This paper discusses line broadening by compositional disorder and by spin–spin exchange interaction between the paramagnetic Cr^{3+} and Gd^{3+} ions in antiferromagnetic $Gd_3Sc_2Al_3O_{12}$ (GSAG) probed using fluorescence line narrowing (FLN) in the absence and presence of a magnetic field. The most intense R_1 lines in Cr^{3+}:GSAG, occurring at $\lambda = 691.2$ nm and 692.4 nm, have halfwidths of $\simeq 32$ cm^{-1}. The linewidths of the FLN spectra at 1.6 K are respectively 19 cm^{-1} and 13 cm^{-1}, much larger than the width of the excitation laser beam (< 0.2 cm^{-1}): thus the contributions to the R_1-line halfwidth from mechanisms of homogeneous and inhomogeneous broadening are approximately equal. In addition, the peaks of the FLN lines are shifted to lower energy from the laser excitation line by $\simeq 8$ cm^{-1}. As the temperature is increased gradually from 1.6 K to 10 K, the FLN peak is shifted to higher energy and is resonant with the excitation above 10 K. In the presence of an external magnetic field the broad FLN spectrum becomes resolvable into three sharp lines with the width of $\simeq 3$ cm^{-1} at $T = 1.6$ K. The peak of the line with maximum intensity is coincident with the excitation energy. The FLN spectrum at $T = 10$ K and $B = 3.46$ T is similar to that at $T = 10$ K in the absence of a magnetic field. The temperature dependence and magnetic field dependence of the FLN spectra are discussed in terms of spin–spin exchange interaction between Cr^{3+} and Gd^{3+} ions in antiferromagnetic GSAG.

1. Introduction

There has been much interest in Cr^{3+}-doped oxide garnets in view of their potential as tunable laser gain media. Both Cr^{3+}:$Gd_3Sc_2Ga_3O_{12}$ (GSGG) and Cr^{3+}:GSAG are useful tunable laser materials for the near-infrared region. In oxide garnets with unit cell structure corresponding to the chemical formula $C_3A_2D_3O_{12}$ (figure 1), Cr^{3+} ions occupy octahedrally symmetric A positions. The rather large rare earth ions (e.g. Y^{3+}, Gd^{3+} etc) occupy the dodecahedral C positions and small ions (e.g. Ga^{3+}, Al^{3+} etc) occupy tetrahedral D positions. Usually solutions of the crystal field Hamiltonian for Cr^{3+} in octahedral sites are represented on Tanabe–Sugano diagrams [1], in which the eigenenergies, E, are plotted as a function of the octahedral crystal field Dq, in units of the Racah parameter B at constant value of the ratio C/B, where the Racah parameters B and C characterize the electron–electron interaction. The ordering of the electronic energy levels of the Cr^{3+} ion are determined by the interplay between

† Permanent address: Department of Physics, Gifu University, Gifu 501-11, Japan.
‡ Now at: Department of Electronic and Computer Engineering, Gifu University, Gifu 501-11, Japan.

0953-8984/92/357307+10$04.50

the strength of the octahedral crystal field and the Racah parameters. The energy levels consist of the $^4A_2$ ground state and the ^2E, $^2T_1$, $^4T_2$ and $^4T_1$ excited states. In general vibrationally broadened $^4A_2 \longrightarrow {}^4T_2$ and $^4A_2 \longrightarrow {}^4T_1$ absorptions are observed at wavelengths in the visible region. Much weaker sharp lines are observed due to the spin-forbidden absorption transitions $^4A_2 \longrightarrow {}^2E$, $^2T_1$, $^2T_2$. The Cr^{3+}-doped Gd-based garnets have been much studied in view of the closeness in energy terms of the lowest-lying excited states ^2E and $^4T_2$. Furthermore, in GSGG the separation of states, $\Delta E = E(^4T_2) - E(^2E)$ is small and positive at low temperatures (+50 cm^{-1} at 1.6 K), and negative (−70 cm^{-1}) at room temperature as a consequence of lattice expansion [2, 3]. The photoluminescence spectrum is a superposition of a broad $^4T_2 \longrightarrow {}^4A_2$ band and the $^2E \longrightarrow {}^4A_2$ R line and its vibronic sideband at low temperature.

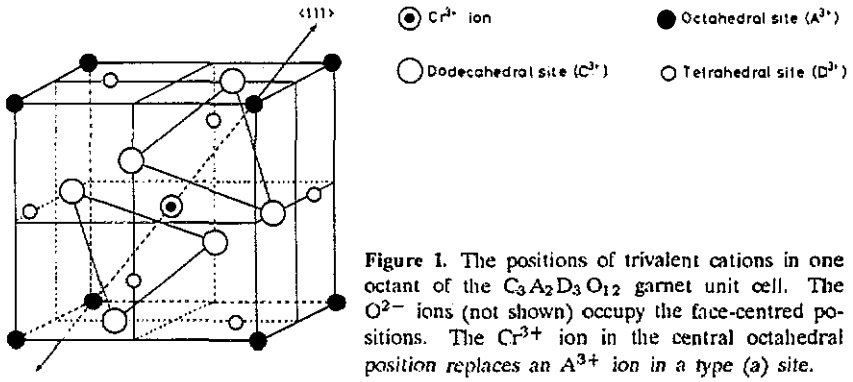

Figure 1. The positions of trivalent cations in one octant of the $C_3A_2D_3O_{12}$ garnet unit cell. The O^{2-} ions (not shown) occupy the face-centred positions. The Cr^{3+} ion in the central octahedral position replaces an A^{3+} ion in a type (a) site.

Depending upon growth conditions, oxide garnets will accommodate a small degree of non-stoichiometry which at the microscopic level is reflected in the composition of the unit cell [4–6]. Deviations from the stoichiometric composition produce different crystal field sites, which result in multiple, inhomogeneously broadened $^2E \longrightarrow {}^4A_2$ (R-line) transitions. For example in GSGG the Ga^{3+} ions, normally resident at tetrahedral D positions, may to some extent occupy the octahedral A (i.e. Sc^{3+}) positions. Since Ga^{3+} is smaller than Sc^{3+} the R lines of Cr^{3+} in such unit cells are shifted to shorter wavelengths. In GSAG, Marshall *et al* [4], identified three sites. The a site is due to Cr^{3+} ions occupying octahedral sites in stoichiometric unit cells. In the b site, a Sc^{3+} ion substitutes for one of the six nearest neighbour Al^{3+} ions in tetrahedral sites and in the c site Al^{3+} substitutes for Sc^{3+} in one of the eight nearest neighbour octahedral sites. The net result is three R_1 lines at wavelengths $R_1(a) = 691.2$ nm, $R_1(b) = 692.4$ nm and $R_1(c) = 689.8$ nm, with intensities proportional to the Cr^{3+} occupancy of the unit cells with the different compositions. These zero-phonon lines have halfwidths of $\simeq$ 30–35 cm^{-1}, much broader than the comparable lines (halfwidth $\simeq$ 12 cm^{-1}) in Cr^{3+}:GSGG crystals grown using the same Czochralski technique.

The Gd-based garnets $Gd_3Ga_5O_{12}$ (GGG), GSAG and GSGG are antiferromagnetic crystals, in which the weaker the octahedral crystal field at the Cr^{3+} site, the lower is the Néel temperature. In GGG the Néel temperature is 0.5 K. The Cr^{3+} R lines in the garnets are broadened homogeneously by superexchange interaction between the Cr^{3+} and the nearest neighbour Gd^{3+} ion. A similar broadening of the R line in $GdAlO_3$, where the Néel temperature is 3.5 K and the exchange constant is

2.1 cm^{-1}, was observed at low temperature [7]. The R_1 line in $GdAlO_3$ is split into four components at 4.2 K, each component being due to one of the four $M_S = \pm\frac{3}{2}$, $\pm\frac{1}{2}$ spin levels of the Cr^{3+} ion. That no splitting of the R_1 line is resolved in GSAG suggests a smaller exchange constant than in $GdAlO_3$.

This paper reports the splitting of the FLN line of GSAG at 1.6 K in a magnetic field. The results are discussed in terms of the relative magnitudes of the exchange and Zeeman interactions.

2. Experimental techniques

Single-crystal boules of Cr^{3+}-doped GSAG were grown by the Czochralski technique from melts synthesized in iridium crucibles from high-purity oxides. The Sc/Al ratio was chosen to give a crystal with approximate composition $Gd_3Sc_{2.4}Al_{2.6}O_{12}$, containing some 2×10^{20} Cr^{3+} ions cm^{-3}. Experimental samples were cut and polished to dimensions of $8 \times 2 \times 1$ mm^3, and placed at the centre of a superconducting solenoid which generated fields up to 3.5 T. The long dimension was parallel to the $\langle 111 \rangle$ crystal axis, the shorter dimensions being parallel to directions in the $\{111\}$ plane. Photoluminescence spectra were excited using the 488 nm and/or 514 nm lines from a Spectra-Physics 2020-05 Ar^+ line, the beam being focused onto the sample as it propagated along the direction of the magnetic field. The emission from the rear surface of the sample was collected along the magnetic field direction also. Both excitation light and luminescence were chopped at frequencies up to 3 kHz and the emitted light detected after a short time delay with the excitation light cut off to eliminate scattered radiation. The photoluminescence from the sample was focused onto the entry slits of a one-metre grating monochromator. The grating was blazed at 500 nm with 1200 lines mm^{-1}. The emitted radiation was detected at the exit slit of the monochromator with a GaAs photomultiplier tube. The signal current from the phototube was amplified by a current amplifier and measured using a lock-in amplifier and boxcar integrator. The choppers also provided timing signals, so that the phase and intensity of the luminescence signal could be compared by the lock-in amplifier and integrated by the boxcar.

In FLN experiments the excitation beam was obtained from a Spectra-Physics 380D ring dye laser, using a DCM dye pumped by the all lines output from the Ar^+ laser. The single-mode output from the ring dye laser could be tuned over the wavelength range 680–715 nm, with a maximum output at the peak wavelength of $\simeq 250$ mW. The FLN measurements were made at temperatures in the range 1.6–15 K at magnetic fields of 0–3.5 T. A field homogeneity of better than one part in 10^{-4} was maintained over the volume of the sample. Although the laser linewidth is less than 0.1 cm^{-1}, the system resolution was only 1 cm^{-1}.

3. Experimental results

3.1. FLN measurements in zero magnetic field

Excitation of Cr^{3+}:GSAG samples at $T = 10$ K using the 488 nm line from the Ar^+ laser results in a spectrum with R lines at 689.8 nm, 691.2 nm and 692.4 nm, together with vibronic sidebands and the broad $^4T_2 \longrightarrow {}^4A_2$ band. The dominant R lines $R_1(a)$ and $R_1(b)$, in figure 2 have peak wavelengths of 691.2 nm and 692.4 nm and

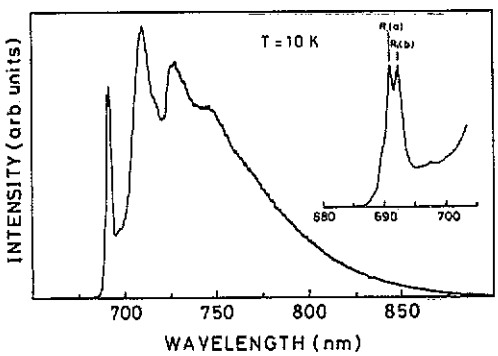

Figure 2. Emission spectrum observed at 10 K and with the 488 nm excitation.

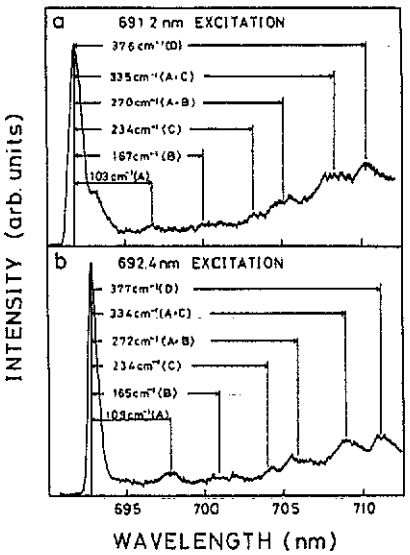

Figure 3. Resonant and non-resonant FLN spectra observed at 10 K and with (*a*) the 691.2 nm excitation at the R_1(a) line and (*b*) the 692.4 nm excitation at the R_1(b) line.

linewidths of $\simeq 32$ cm^{-1}. In other oxides the linewidth of the R lines may be less than 1 cm^{-1}, implying that there is significant inhomogeneous broadening in the Cr^{3+}:GSAG spectra. The FLN spectra shown in figure 3 were measured at 1.6 K and with excitation wavelengths of (a) 691.2 nm and (b) 692.4 nm respectively. The FLN widths at 691.8 nm and 692.7 nm are 19 cm^{-1} and 13 cm^{-1} respectively, indicating that the inhomogeneous and homogeneous broadenings make approximately similar contributions to the widths of the R lines. Note that the FLN peaks are not resonant with the excitation but are shifted to longer wavelengths. At 1.6 K the FLN peak excited at 691.2 nm is shifted to 691.8 nm and that excited at 692.4 nm is shifted to 692.7 nm, figure 4. The FLN spectra are asymmetric in shape having pronounced long-wavelength tails. The temperature dependence of the FLN peak shift excited at 692.4 nm is shown in figure 5: as the temperature is increased, the peak is shifted to shorter wavelengths and at 8 K the FLN peak is resonant with the excitation wavelength. Above 8 K, the lineshape becomes more symmetric in shape because the optical absorption from the thermally populated higher energy levels of the ground state excites the higher-energy Cr^{3+} ion sites. There is no broadening of the FLN lines in the temperature range 1.6–12 K for either 691.2 nm and 692.4 nm excitations.

The vibronic structure in figure 3 is shifted to lower energies from R lines, and has specific phonon energies, identified in figure 3 by the different one-phonon lines A, B, C and D. For FLN lines excited at 691.2 nm the one-phonon components A, B, C and D have identical energies: $E_A = 103$ cm^{-1}, $E_B = 167$ cm^{-1}, $E_C = 234$ cm^{-1} and $E_D = 376$ cm^{-1}. There are also in each spectrum phonon-combination peaks A + B = 270 cm^{-1} and A + C = 335 cm^{-1}. Figure 3(*b*) also shows that for 692.4 nm excitation energy is transferred from the 691.2 nm emission system to that at 692.4 nm since the lower energy FLN line at 692.7 nm is also observed.

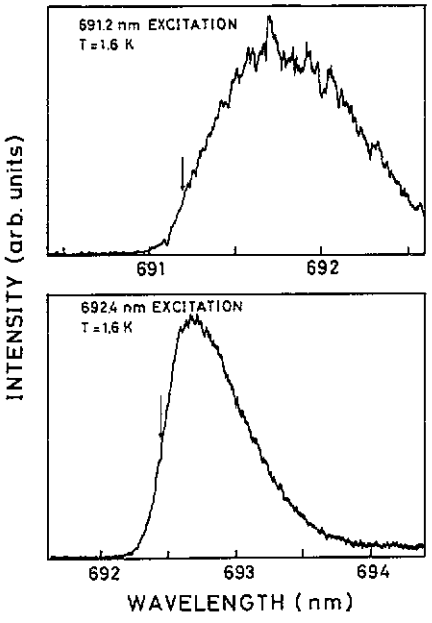

Figure 4. Resonant FLN observed at 1.6 K and with (upper panel) the 691.2 nm excitation and (lower panel) the 692.4 nm excitation. The arrows indicate the excitation energy.

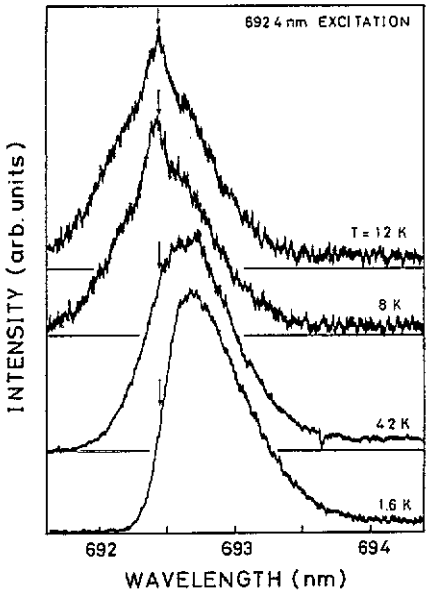

Figure 5. Temperature dependence of FLN spectra with the 692.4 nm excitation. The arrows indicate the excitation energy.

3.2. FLN in a magnetic field

Figure 6 shows the effect on the 692.7 nm FLN line of an external magnetic field with the GSAG sample held at 1.6 K. As the magnetic field is increased, splittings into three components can be observed. A clear separation of the components becomes evident at $B = 0.87$ T. Further increases in the magnetic field lead to further slight increases in the separations between the components and a narrowing of each line. However, when the magnetic field reaches 3.46 T, the separation between the components saturates. Note that the splitting pattern never extends beyond the lineshape of the zero-field spectrum. Note also that the application of an intense magnetic field tends to counteract the FLN peak shift relative to excitation wavelength. The larger the field the smaller the peak shift: for a magnetic field of 3.46 T the FLN peak position is at the excitation wavelength. The magnetic field splitting patterns of the two FLN lines with the peaks at 691.8 nm and 692.7 nm have different separations between components. For the line at 691.8 nm, the separations between successive components in a magnetic field of 3.4 T are almost the same and equal to 9.5 cm^{-1}. The linewidth of the short wavelength component at 691.2 nm is 3.1 cm^{-1}. At the same field the separations between the three magnetic field components of the line at 692.7 nm are also identical and equal to 8.7 cm^{-1}. The linewidth of the short-wavelength component at 692.4 nm is 2.8 cm^{-1}. When with the field at 3.46 T the temperature is increased above 1.6 K there is a gradual broadening of the components until at temperatures above 12 K a single line is observed resonant with the laser excitation (figure 7).

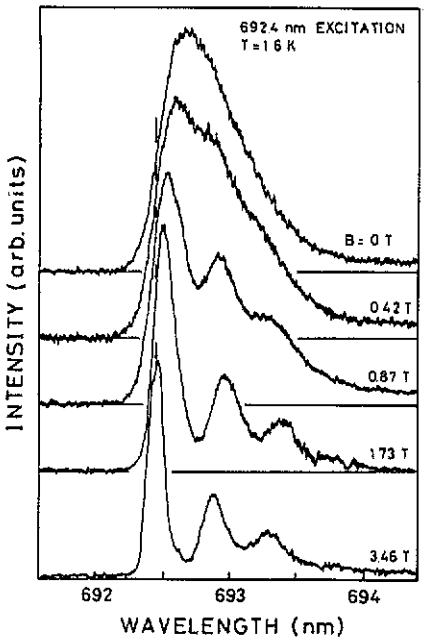

Figure 6. Magnetic field dependence of FLN spectra at 1.6 K and with the 692.4 nm excitation. The arrows indicate the excitation energy.

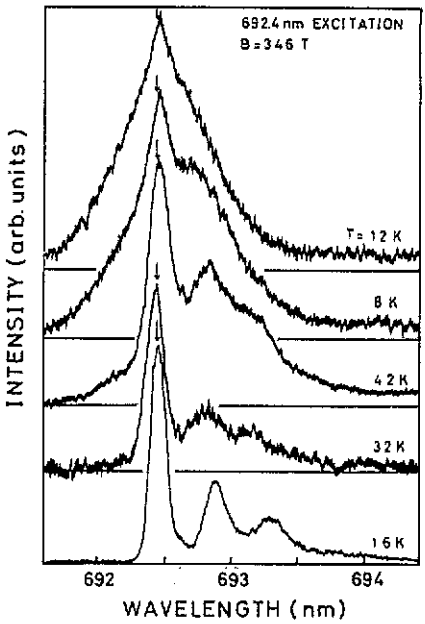

Figure 7. Temperature dependence of FLN spectra with the magnetic field $B = 3.46$ T.

4. Discussion

The authors have shown in earlier publications that $Y_3Ga_5O_{12}$ (YGG), GSGG and GSAG all support different levels of compositional disorder [2, 4]. At least in GSGG and GSAG the congruent melting composition is not the ideal chemical formula, although the tolerance level for non-stoichiometry is rather less in GSGG than in GSAG [2, 4–6, 8, 9]. In the present study there are two consequences of this compositional disorder. First of all there is a multiplicity of R lines. Secondly, non-stoichiometry in unit cells remote from the individual Cr^{3+} ions will lead to inhomogeneous broadening of the R lines. The measured halfwidths of the R line are of order 32 cm^{-1} for both the 691.2 nm and 692.4 nm lines. In FLN measurements below $T = 2$ K these lines are shifted to 691.8 nm and 692.7 nm, respectively, and the widths reduced to 19 cm^{-1} and 13 cm^{-1}. These results show that approximately half of the normal R line width is due to inhomogeneous broadening by strain and non-stoichiometry. Nevertheless, the homogeneous width of the R lines is much larger than the natural width associated with the radiative decay time. The additional de-phasing process in antiferromagnetic oxides such as the Gd garnets is superexchange between the central Cr^{3+} ion in the unit cell, figure 1, and the six nearest neighbour Gd^{3+} ions.

The exchange interaction is very sensitive to the separation between magnetic ions, in both direct exchange and superexchange via ligand ions. In view of the dependency of the strength of the octahedral crystal field on unit cell dimensions the exchange parameter should follow trends in the value of Dq/B. In GSAG the separation between the central Cr^{3+} ion and the nearby Gd^{3+} ion is too large for direct overlap of the electronic wavefunctions. Instead the Cr^{3+} and Gd^{3+} spins

are coupled by indirect overlap involving the intervening ligand ions. The isotropic spin–spin exchange coupling can be written as

$$H_J = -\mathcal{J} S_{Cr} S \tag{1}$$

where $S_{Cr} = \frac{3}{2}$ in the ground state and $\frac{1}{2}$ in the excited state. The total spin of the six interacting Gd^{3+} ions, $S = \Sigma_{i=1}^{6} S_i$ where $S_i = \frac{7}{2}$, takes integral total spin values ranging from zero to 21. The total number, N_S, of ways of forming a state of total spin S from the six gadolinium ions is listed in table 1 [7]. If the exchange constant, $\mathcal{J}$, is small each of the $M_S = \pm\frac{3}{2}, \pm\frac{1}{2}$ levels of the $S_{Cr} = \frac{3}{2}$ ground state is split into a quasi-continuous band of exchange-coupled sub-levels having total spin quantum numbers $\tilde{S}$ given by $\tilde{S} = |S + \frac{3}{2}|$, $\tilde{S} = |S + \frac{1}{2}|$, $\tilde{S} = |S - \frac{1}{2}|$, $\tilde{S} = |S - \frac{3}{2}|$. In the garnets the ^2E state is split by the spin–orbit coupling and trigonal distortion into $2\overline{A}$ and $\overline{E}$ levels, of which $\overline{E}$ is lowest. In this $^2E(\overline{E})$ level there are two sub-bands, one corresponding to $\tilde{S} = |S + \frac{1}{2}|$ and the other to $\tilde{S} = |S - \frac{1}{2}|$. The physical effect of spin–spin exchange is that the Cr^{3+} ions experience a magnetic field of randomly varying strength and direction, so that the Cr^{3+} energy levels are split and shifted in random fashion. This results in a broadening of the spectra, the magnitude of which is determined by the magnitude of the exchange constant, $\mathcal{J}$. Figure 8 shows electron spin density of the ground state as a function of energy, split by exchange interaction, equation (1). The energy unit is the exchange coupling constant, $\mathcal{J}$, which is assumed to be positive. The bars indicate the degeneracy, defined as $(2\tilde{S} + 1)N_S$ of the spin states with total spins, $\tilde{S}$ and S, where values of N_S are listed in table 1.

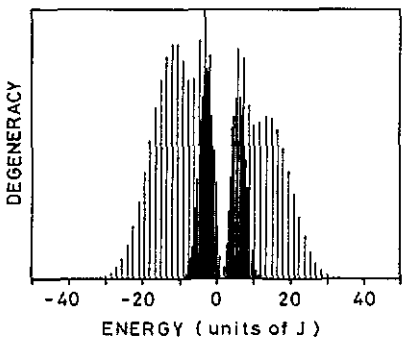

Figure 8. Spin degeneracy of the ground state as a function of energy, split by the exchange interaction, equation (1).

Table 1. Total number of vectors of length S formed by adding together six vectors of length 7/2.

S	0	1	2	3	4	5	6	7	8	9	10
N_S	260	756	1190	1534	1770	1890	1896	1800	1624	1400	1155
S	11	12	13	14	15	16	17	18	19	20	21
N_S	911	685	489	330	210	126	70	35	15	5	1

This situation in Cr^{3+}:GSAG is analogous to the case of Cr^{3+}:$GdAlO_3$ except that in that case there are eight neighbouring Gd^{3+} ions rather than six. For $GdAlO_3$ where $Dq/B \simeq 2.72$, the exchange sub-bands are resolved [7], whereas in GSAG

$Dq/B \simeq 2.55$ they are not. In contrast, rather narrow FLN lines ($\simeq 1.3$ cm^{-1}) are observed in Cr^{3+}:GSGG [10] where $Dq/B \simeq 2.44$. The indirect Cr–Gd exchange constant is then much smaller. That the R_1(a) and R_1(b) lines in Cr^{3+}:GSAG have different halfwidths in FLN spectroscopy also reflects the different local dimensions in the presence of non-stoichiometry. The different values of Dq/B, can be estimated from [2, 8, 9]

$$E(^2\mathrm{E}) = 7.90B - 1.80B^2/Dq + 3.09C \tag{2}$$

giving for the R_1(a) line $Dq/B = 2.60$ and for the R_1(b) line $Dq/B = 2.57$, and as anticipated from the above discussion, the R_1(a) line has the larger exchange-induced FLN width. Rather similar considerations apply to the case of Cr^{3+}:$Gd_3Ga_5O_{12}$ (GGG) [10–12].

In principle, the shift in the peak position of the FLN line relative to the excitation wavelength may be due to several factors. For Cr^{3+}:GSAG, the shift varies from 6 cm^{-1} to 12 cm^{-1}, which is small compared with the R_1–R_2 separation (54–56 cm^{-1}) [4]. In consequence, the FLN shift is not associated with the excited state splitting, and must be due predominantly to the spin–spin exchange interaction. In the model described above, the $^4A_2$ ground state is split into four bands, and the $^2\mathrm{E}(\bar{\mathrm{E}})$ excited state is split into two bands. Since the Cr–Gd system is in thermal equilibrium with the lattice at 1.6 K, only the lowest band of the ground state is populated. Laser excitation at 1.6 K into sub-levels within the $|^2\mathrm{E}, S + \frac{1}{2}\rangle$ band will be followed by non-radiative relaxation to the lowest levels of the $|^2\mathrm{E}, S + \frac{1}{2}\rangle$ subband, from which the fluorescence transitions will access all levels within the $|^4A_2, S - \frac{1}{2}\rangle$, $|^4A_2, S + \frac{1}{2}\rangle$ and $|^4A_2, S + \frac{3}{2}\rangle$ subbands. These transitions are allowed by the selection rule that the total spin, S, of gadolinium ions is conserved and the conservation of the total spin $\tilde{S}$ breaks down as a consequence of spin–orbit interaction between $^2\mathrm{E}$ and $^4T_2$. Since most of these levels have lower energy separations from the $^2\mathrm{E}(\bar{\mathrm{E}})$ level than the energy of the exciting radiation, the position of the FLN line is shifted to lower energy from the excitation. Essentially the shift is caused by the multiplicity of overlapping exchange levels in the $^4A_2$ subbands.

The line at 691.2 nm comes from Cr^{3+} ions at stronger crystal field sites relative to that at 692.4 nm, and according to the model the exchange interaction for this line is stronger than that for 692.4 nm line. Hence the position shift from the 691.2 nm excitation wavelength is expected to be larger than that at 692.4 nm, in accord with experimental results. That the peak positions of the FLN line shift to shorter wavelengths with increasing temperature can be explained by the fact that the higher levels of the ground state manifold become increasingly populated and optical absorption transitions from these higher levels to the excited state will occur at Cr^{3+} sites with higher energy resulting in emission at shorter wavelengths. The width of the resonant lines is still quite broad because the exchange interaction remains effective.

The splitting and narrowing of the FLN R lines are compelling evidence that the application of an external magnetic field removes the random spin–spin exchange interaction, thereby reducing its contribution to the width of FLN lines. Since the spectroscopic splitting factors, g, in the ground states of Cr^{3+} and Gd^{3+} ions are isotropic and approximately two, the maximum Zeeman splitting caused by the removal of spin degeneracy by the external magnetic field is much smaller than the splittings of 9.5 cm^{-1} and 8.7 cm^{-1} observed for the 691.8 nm and 692.7 nm lines, respectively. These splittings may contain contributions from the Zeeman energy, 3.2 cm^{-1} ($B \simeq 3.5$ T) and zero-field splitting of the Cr^{3+} ground state. For

Cr^{3+}-doped Al_2O_3, YAG and YGG, the zero-field fine structure splittings, $2D$, are 0.38 cm^{-1}, 0.53 cm^{-1} and 0.7 cm^{-1}, respectively. The strength of the octahedral crystal field decreases in this order. Since in GSAG the crystal field is weaker still, the zero-field splitting is expected to be of order 1 cm^{-1}. Thus the spin–spin fine structure interaction of the Cr^{3+} ion is not large enough to contribute significantly to the homogeneous line broadening, and we must consider the spin–spin interaction between Cr^{3+} and Gd^{3+} ions in GSAG in the presence of a magnetic field. The spin-Hamiltonian including Zeeman and spin–spin exchange interactions is given by

$$H = g_{Cr}\mu_B S_{Cr}\cdot B + g_{Gd}\mu_B S\cdot B - \mathcal{J} S_{Cr}\cdot S \tag{3}$$

where $g_{Cr} \approx g_{Gd} \simeq 2.00$, μ_B is the Bohr magneton, B is the external magnetic field, $|S_{Cr}| = \frac{3}{2}$ and $|S| = 0, 1, 2, 3, \ldots, 21$. $\tilde{S}$ is a good quantum number represented by $\tilde{S} = S + S_{Cr} = |S+\frac{3}{2}|\,|S+\frac{1}{2}|, |S-\frac{1}{2}|$ and $|S-\frac{3}{2}|$ in equation (3). The lowest energy levels of the ground and excited state spin sub-bands, split by the spin–spin exchange interaction in the absence of a magnetic field, are defined by $|^4A_2, \tilde{S} = 21 + \frac{3}{2}\rangle$ and $|^2E, \tilde{S} = 21 + \frac{1}{2}\rangle$, respectively. When the magnetic field is applied and the magnetic quantum number, $M_{\tilde{S}}$, added, the spin degenerate state of $|^4A_2, \tilde{S} = 21 + \frac{3}{2}, M_{\tilde{S}}\rangle$ splits into 46 magnetic sub-levels, the lowest energy level of which corresponds to $M_{\tilde{S}} = -22.5$. Transitions from the excited state $|^2E, \tilde{S}, M_{\tilde{S}}\rangle$ to the ground states $|^4A_2, \tilde{S}, M_{\tilde{S}}\rangle$ occur provided that the total spin S and magnetic angular component M_S of six Gd ions are conserved.

The three components in figure 6 are due to the transitions from $|^2E, \tilde{S} = 21 + \frac{1}{2}, M_{\tilde{S}} = -(21 + \frac{1}{2})\rangle$ to $|^4A_2, \tilde{S} = 21 + \frac{3}{2}, M_{\tilde{S}} = -(21 + \frac{3}{2})\rangle, |^4A_2, \tilde{S} = 21 + \frac{1}{2}, M_{\tilde{S}} = -(21 + \frac{1}{2})\rangle$, and $|^4A_2, \tilde{S} = 21 - \frac{1}{2}, M_{\tilde{S}} = (21 - \frac{1}{2})\rangle$; the $|^2E\tilde{S} = 21 + \frac{1}{2}, M_{\tilde{S}} = -(21 + \frac{1}{2})\rangle$ to $|^4A_2, \tilde{S} = 21 - \frac{3}{2}, M_{\tilde{S}} = -(21 - \frac{3}{2})\rangle$ transition is forbidden. The energy separations between these three transitions are represented by

$$\begin{aligned} E(\tfrac{1}{2} \rightarrow \tfrac{3}{2}) - E(\tfrac{1}{2} \rightarrow \tfrac{1}{2}) &= 2\mu_B B + 22.5\,\mathcal{J} \\ E(\tfrac{1}{2} \rightarrow \tfrac{1}{2}) - E(\tfrac{1}{2} \rightarrow -\tfrac{1}{2}) &= 2\mu_B B + 21.5\,\mathcal{J}. \end{aligned} \tag{4}$$

The energy separations of 9.5 cm^{-1} and 8.7 cm^{-1} observed for the 691.8 nm and 692.7 nm lines, respectively, can be used to estimate the exchange coupling constants $\mathcal{J} = 0.28$ cm^{-1} and 0.25 cm^{-1}, respectively. These values are one order of magnitude smaller than in $GdAlO_3$ ($\mathcal{J} = 2.1$ cm^{-1}) [7]. This result is consistent with the crystal field of Cr^{3+} in GSAG being smaller than that in $GdAlO_3$.

For both FLN lines, the linewidth decreases with increasing magnetic field, because the stronger the magnetic field the more effective is it in removing the randomness of the spin–spin exchange interaction. In consequence, the quasi-continuous sub-bands of the ground and excited states are resolved by the Zeeman splitting energy. The most intense peak in figure 5 is resonant with the laser at high field, because at low temperature ($kT <$ Zeeman energy), the transitions between $|^4A_2, \tilde{S} = 21 + \frac{3}{2}, M_{\tilde{S}} = -(21 + \frac{3}{2})\rangle$ and $|^2E, \tilde{S} = 21 + \frac{1}{2}, M_{\tilde{S}} = -(21 + \frac{1}{2})\rangle$ are the same for both absorption and emission processes.

As the temperature is increased at constant magnetic field $B = 3.46$ T (figure 7) the individual components broaden appreciably. However, at 4.2 K a weak component is observed at $\simeq 692.3$ nm, on the short-wavelength edge of the most intense component. At still higher temperatures the individual components cannot

be resolved and at 12 K only a single broad band is observed. Indeed the lineshape and peak position (figure 7) is identical with that measured in zero magnetic field at $T = 12$ K (figure 5). These behaviours can be explained as follows: as the temperature is raised, higher-lying levels of the ground state are thermally populated. The laser can excite the several Cr^{3+} sites with different crystal fields, through the transitions between the different ground and excited spin levels, and the higher energy levels of the excited state are also thermally populated. These effects produce the emission at shorter wavelengths than the laser excitation wavelength and the FLN lineshape becomes more symmetric. These effects are dominant when the thermal energy (kT), is larger than the Zeeman splitting energy ($\Delta M_{\tilde{S}}\, g\mu_B B$) and the FLN lineshape becomes more symmetric.

5. Conclusions

FLN studies of the R lines of Cr^{3+} ion in GSAG show that inhomogeneous broadening by strain and compositional disorder contribute equally with homogeneous broadening by spin–spin exchange interactions between Cr^{3+} ions and Gd^{3+} to the observed lineshape at temperatures in the range 1.4–15 K. The application of magnetic fields up to 3.46 T reduces the line-broadening effects associated with the exchange-induced random, fluctuating magnetic fields such that resolvable splittings may be observed. The experimental results are in accord with a phenomenological model, in which the energy levels of the Cr^{3+} ions are exchange-coupled to six neighbouring Gd^{3+} ions.

Acknowledgments

This work has been supported through Research Grant RG/E/94173 from the Science and Engineering Research Council. Y Gao was a Visiting Scholar supported by the University of Strathclyde for the duration of his PhD studies. C Ogihara and M Yamaga were supported as Visiting Research Fellows also by the University of Strathclyde.

References

[1] Tanabe Y and Sugano S 1958 *J. Phys. Soc. Japan* **13** 394
Sugano S, Tanabe Y and Kamimura H 1970 *Multiplets of Transition Metal Ions in Crystals* (New York: Academic)
[2] Henderson B, Marshall A, Yamaga M, O'Donnell K P and Cockayne B 1988 *J. Phys. C: Solid State Phys.* **21** 6187–98
[3] Healy S M, Donnelly C J, Glynn T J, Imbusch G F and Morgan G P 1990 *J. Lumin.* **46** 1–7
[4] Marshall A, O'Donnell K P, Yamaga M, Henderson B and Cockayne B 1990 *Appl. Phys.* A **50** 565–72
[5] Struve B and Huber G 1985 *Appl. Phys.* B **36** 195–201
[6] Healy S M, Donnelly C J, Glynn T J, Imbusch G F and Morgan G P 1989 *J. Lumin.* **44** 65–71
[7] Murphy J and Ohlmann R C 1967 *Optical Properties of Ions in Crystals* ed H M Crosswhite and H W Moos (New York: Wiley) pp 239–50
[8] O'Donnell K P, Marshall A, Yamaga M and Henderson B 1989 *J. Lumin.* **42** 365–73
[9] Henderson B and Imbusch G F 1989 *Optical Spectroscopy of Inorganic Solids* (Oxford: Oxford University Press) ch 9
[10] Monteil A 1990 *J. Phys.: Condens. Matter* **2** 9639–51
[11] Monteil A, Nie W, Madej C and Boulon G 1990 *Opt. Quantum Electron.* **22** S247–57
[12] Monteil A, Ferrari M and Rossi F 1991 *Phys. Rev.* B **43** 3646